# Tunable femtosecond pulse source from 1.6 to 2.3 μm with 100 kW peak power in an all-fiber system

**Peng Wang (王 鹏), Hongxing Shi (师红星), Fangzhou Tan (谭方舟), and Pu Wang (王 璞)***

*National Center of Laser Technology, Institute of Laser Engineering, Beijing University of Technology, Beijing 100124, China*

**Corresponding author: wangpuemail@bjut.edu.cn*

Received May 27, 2016; accepted July 22, 2016; posted online August 30, 2016

We report a simple and compact all-fiber laser system that is capable of generating widely tunable femtosecond pulses from 1.6 to 2.32 μm. The pulses are produced by utilizing the soliton self-frequency shift in a highly nonlinear fiber pumped by an Er-doped mode-locked fiber laser. Two stages of single-clad Tm:fiber amplifiers are used to amplify the pulses to a higher pulse energy of 10.9 nJ with pulse width of 94 fs, and corresponding to peak power of 105 kW at around 1.93 μm. Running a few hours, the all-fiber laser system exhibits exceptional stability with a signal-to-noise ratio as high as 70 dB.

*OCIS codes: 140.3280, 140.3510, 140.3600, 140.7090.*
*doi: 10.3788/COL201614.091405.*

Over the past decade, there has been a growing interest in tunable ultrashort optical pulses that are useful for a number of commercial and scientific applications, including ultrafast spectroscopy, material processing, nonlinear optics, and defense security. In most of the cases so far, the pulses have been realized using solid state lasers or dye lasers with many free space optical elements. However, in the systems using those lasers, it is necessary to control the optical elements with very high precision through complicated adjustments in order to get the stable operation and tune the wavelength of the laser pulse, and the whole system is rather large and not easy to control, thus the overall system cost is rather high. Meanwhile, the tuning range remains limited by the bandwidth of the gain medium.

Recently, ultrafast fiber laser technology has progressed remarkably and the performance is comparable to standard solid-state lasers[1,2]. The tunable ultrashort pulses can be produced by utilizing the soliton self-frequency shift[3] (SSFS) in silica fibers based on compact fiber lasers with excellent beams and pulse quality, wide tunable range, high stability and turn-key operation. With SSFS, several groups have succeeded in the demonstration of a wavelength tunable laser system for short pulse generation[4–12]. Examples of those tunable ultrashort pulses source were realized by using the diameter reduced type of polarization maintaining fiber and passively mode-locked Er-doped fiber laser for generating tunable optical pulses from 1.56 to 2.03 μm[7]. Furthermore, shifting of the wavelength from 1.58 to 2.07 μm was achieved for 100 fs optical pulses in a 1-m-long high nonlinear fiber (HNLF)[8]. In addition, pulses from a femtosecond Er:fiber oscillator and a diode-pumped Er-doped fiber preamplifier at 1.6 μm are converted in silica fiber up to 2 μm and are amplified in Tm-doped silica fiber to generate two-color ultrashort pulses with a tunable wavelength up to 2.3 μm[10]. Apart from that, people can also obtain short wavelength tunable pulses called dispersion waves (DWs) based on this method. In 2010, Andrianov *et al.* got a pulse with a duration as short as 85 fs and an averaged power of 200 mW based on nonlinear wavelength conversion of 1.56 μm ultrashort Er:fiber laser pulses to the 1 μm range in a short span of dispersion-shifted silica fiber[13].

At present, the wavelength tunable ultrashort pulse sources are usually used to seed high-power amplifiers or optical parametric amplifiers, etc.[14–19]. For instance, such schemes were utilized by Coluccelli *et al.* for seeding single-clad Tm-Ho:fiber amplifier to generate high-power sub-100-fs pulses around 1.9 μm with complicated spatial structures[16]. In addition, Imeshev *et al.* have reported the generation of tunable femtosecond optical pulses at around 2 μm by large mode area (LMA) double-clad Tm-doped fiber without an external pulse compressor[17]. Although they obtained an 108 fs pulse with 230 kW peak power, the method of pumping was complex, accompanied with instability, and the use of cladding-pumped LMA fiber raised the cost.

Here, we report a simple and compact all-fiber laser system that generates tunable femtosecond optical pulses from 1.6 to 2.32 μm with an Er-doped mode-locked fiber laser based on telecom components and a silica-based highly nonlinear fiber. In the meantime, the use of a single-clad Tm-doped fiber amplifier allows the production of high-power femtosecond pulses around 1.93 μm without an external pulse compressor. We obtain pulse trains at a repetition frequency of 32.9 MHz with an average power of 360 mW, pulse energy of 10.9 nJ, duration of 94 fs, and corresponding peak power of 105 kW.

One should note that the magnitude of the wavelength shift is up to 720 nm. Furthermore, we can obtain femtosecond pulses with a peak power of 105 kW based on

 

single-clad Tm-doped fiber amplifier in an all-fiber system without any free space optical components.

The experimental setup of the all-fiber laser system is shown in Fig. 1. It consists of a passively mode-locked Er:fiber master oscillator, a diode-pump Er-doped fiber amplifier, a single-mode fiber (SMF) used as a nonlinear pulse compressor, a silica-based HNLF for wavelength conversion, two stages of single-clad Tm-doped fiber power amplifier, and an ultrahigh numerical aperture (UHNA) fiber used as dispersion compensation fiber (DCF) for shortening the output pulses to sub-100-fs.

In the HNLF front end, an in-house built all-fiber master oscillator passively mode-locked by using nonlinear polarization rotation (NPR) delivers 490 fs optical pulses with a 6.9 nm spectral bandwidth centered at 1.56 μm at a fundamental frequency of 32.9 MHz. The optical pulses pass through an optical isolator for preventing back reflections and are then amplified in a 3-m-long customized Er-doped fiber with a mode field diameter of 5.7 μm at 1550 nm, an absorption of 16.5 dB/m at 980 nm, and a normal dispersion of 14.3 $ps^2$/km at 1.55 μm. Subsequently, the SMF lengths inside a 980/1550 wavelength division multiplex (WDM) coupler are carefully chosen to compress the optical pulses. The pulse width after compression exhibits a strong dependence on the output power due to the use of SMF as a nonlinear pulse compressor. Figure 2 shows the change of average output power and pulse width at the output along with the backward pump power.

Next, the compressed pulses are directly coupled into HNLF with a core diameter of 2 μm for wavelength conversion. The HNLF has the zero dispersion wavelength of 1453 nm and its nonlinear coefficient is much higher than SMF-28 because of a smaller effective mode area. As the coupling power and pulse width vary, the wavelength of the generated optical pulses is shifted arbitrarily and continuously. Figure 3(a) shows the observed optical spectrum at the output of the 5-m-long HNLF when the coupling power is about 26 mW with 90 fs pulse width. We obtain optical pulses centered at 2.11 μm with a spectral width of 33 nm corresponding to 142 fs pulse width under the assumption of the $sech^2$ pulse shape. If we further increase the injected power in the HNLF fiber

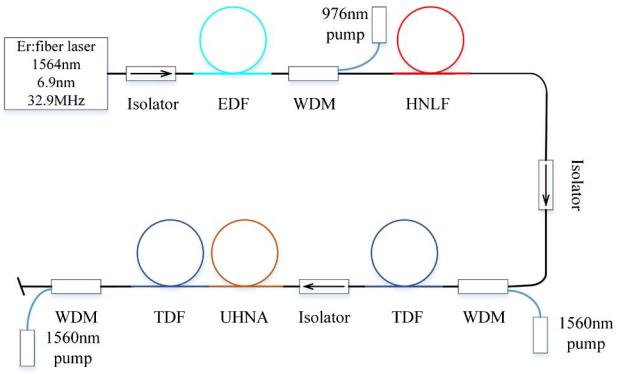


Fig. 1. Optical layout of the experimental setup.

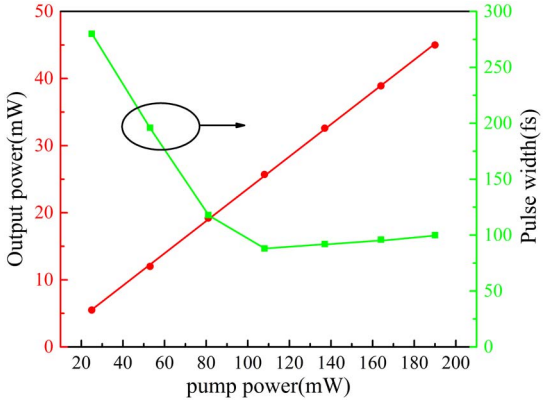


Fig. 2. Average output power and pulse width of the amplified pulses as a function of pump power.

the output will turn into a supercontinuum emission. In order to obtain the longest wavelength optical pulses, we increase the coupling power up to 45 mW with 7-m-long HNLF. An example of an optical pulse at 2.32 μm with 31 nm spectral width that perfectly fits the Cr:ZnSe amplification bandwidth is presented in Fig. 3(b).

Figure 4 shows the characteristics of the wavelength shift of the first optical pulse as a function of the fiber input power in a 7-m-long HNLF. We can see from the picture that the wavelength of the generated soliton pulse is shifted continuously toward the long wavelength side as the fiber input power is increasing. But the wavelength conversion saturates at 2.32 μm and the speed of the shift decreases gradually because of the onset of the infrared absorption edge of the silica glass and a decrease of the

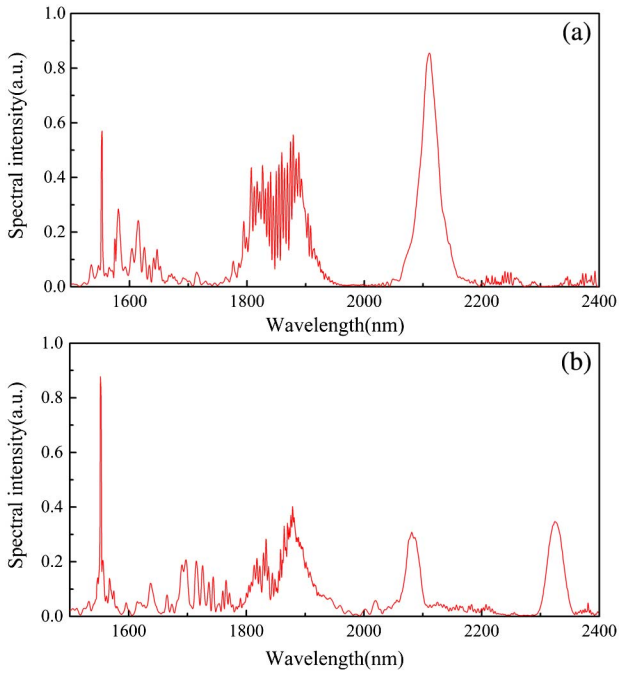


Fig. 3. Output spectrum measured at the fiber output with different pump power and HNLF length (a) 26 mW, 5 m and (b) 45 mW, 7 m.

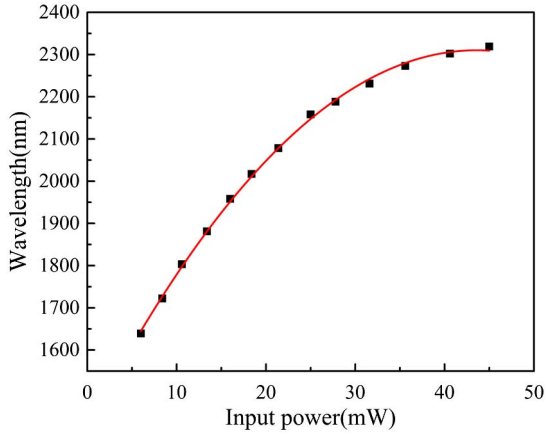


Fig. 4. Characteristics of wavelength shift of soliton pulses in function of fiber input power (dots with experimental data) and arbitrarily fit (red curve).

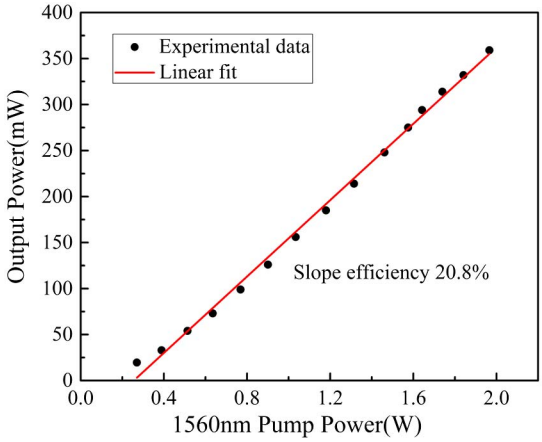


Fig. 5. Average output power as a function of launched 1560 nm pump power (dots with experimental data) and linear fit (red curve).

pulse intensity owing to the increase of the anomalous dispersion with the decrease of the nonlinear coefficient along the shifted wavelength. The conversion efficiency to the optical pulses at 2.32 μm is about 10%. One should note that higher conversion efficiencies can be expected when optimum fiber designs are used and even larger wavelength shifts can be expected when fluoride fiber is used to overcome the absorption edge of silica.

To verify the tunability and stability of the optical pulses, two stages of single-clad Tm-doped fiber amplifiers are used to boost the power level further in the 2 μm region.

First, the coupling power is optimized to pump the 7-m-long HNLF for generating 1.95 μm optical pulses in order to match the Tm-doped fiber gain bandwidth. The seed pulses are then coupled into a 2 m length of single-clad Tm-doped fiber to filter out the long wavelength element and amplified up to 10 mW average power at 1.95 μm. The Tm-doped fiber used in the amplifier has a core/cladding diameter of 9/125 μm, and a numerical aperture (NA) of 0.16 with an absorption coefficient of 13 dB/m at 1550 nm. The group velocity dispersion (GVD) of the fiber is dominated by the negative contribution from the host silica material and has been estimated to be $-70$ ps$^2$/km. Next, the optical pulses are stretched by UHNA fiber to compensate the anomalous dispersion in the SMF and amplifier. The UHNA has a core/cladding diameter of 2.2/125 μm, and an NA of 0.35 with a GVD of 90 ps$^2$/km.

Finally, the 3-m-long main amplifier is made of single-clad Tm-doped fiber, similar to the previous. An Er-doped fiber laser with a coupled power of 2.0 W at 1560 nm is used to pump the amplifier, which resulted in a maximum output power of 360 mW at around 1931 nm, as shown in Fig. 5. The slope efficiency with respect to the pump power is 20.8%, as represented by the red line in Fig. 5.

Before the UHNA fiber, the average power is 10 mW, the full width at half-maximum (FWHM) pulse width at the output of the amplifier is measured at 9 ps with an autocorrelator and the autocorrelation trace with

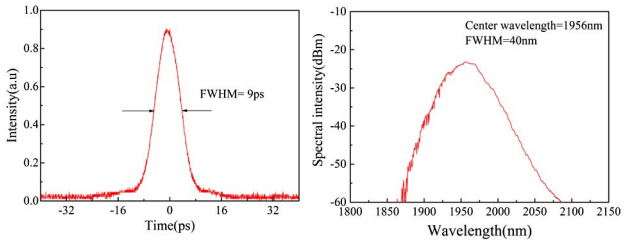


Fig. 6. Autocorrelation trace (left) and spectrum (right) of uncompressed pulses.

corresponding spectrum are shown in Fig. 6. The wide pulse width is due to the chirp accumulated during the propagation in the silica fiber for the large amount of anomalous dispersion above 1600 nm. After adding 8-m-long UHNA fiber, we obtained femtosecond optical pulses with 10.9 nJ pulse energy at 1931 nm. Assuming a sech$^2$ pulse profile, we estimate a pulse width of 94 fs with a 10% pedestal content and a time bandwidth product of 0.53. Subtracting the pedestal content from the total pulse energy, we estimate the pulse peak power at the output of amplifier as 105 kW. An autocorrelation of the typical compressed output pulses and corresponding spectrum is shown in Fig. 7. Spectrum reshaping inside the amplifier is responsible for the nonlinear effect at the

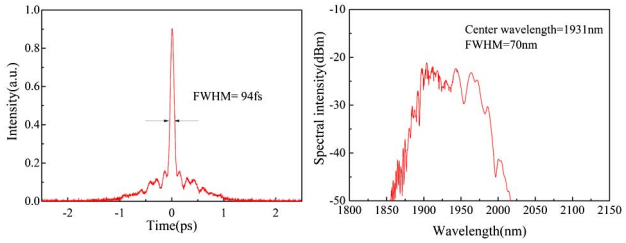


Fig. 7. Autocorrelation trace (left) and spectrum (right) of compressed pulses.

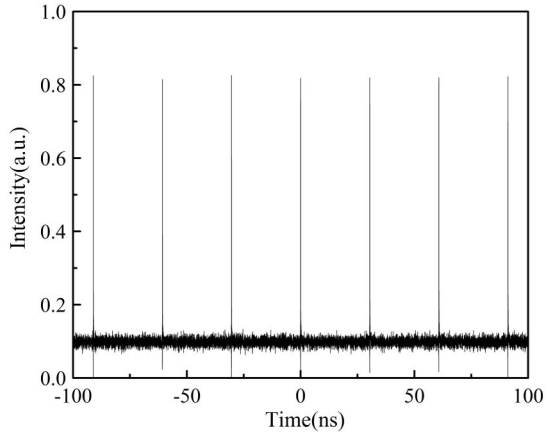


Fig. 8. Recorded output pulse train.

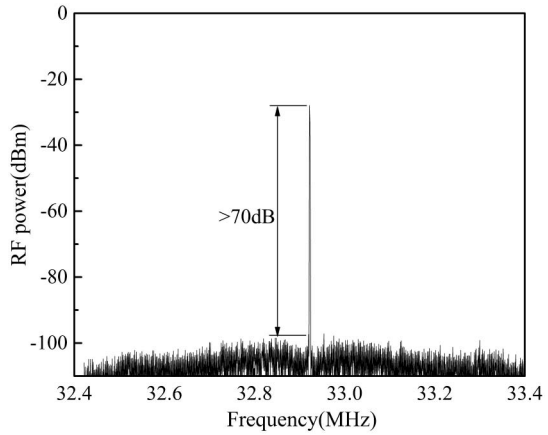


Fig. 9. RF spectrum of the compressor pulses recorded with 510 Hz RBW.

highest power levels and the center wavelength is shifted to a shorter wavelength mainly due to the gain bandwidth of Tm-doped fiber in the short wavelength region. The autocorrelation of the compressed pulses displays a high pulse quality despite the high amount of self-phase modulation in the Tm amplifier.

The compressed output pulse train observed in a high-speed oscilloscope is shown in Fig. 8. The pulses are equally separated by around 30 ns, corresponding to a 32.9 MHz repetition frequency. No signs of double-pulsing or pulse breaking are observed.

All the fibers are fusion spliced to make the system mechanically stable. Running a few hours at maximum average power, the all-fiber laser system exhibits exceptional stability with overall power fluctuations as low as 0.5%. In order to further verify the stability of the laser system, we record the RF spectrum with 510 Hz resolution bandwidth (RBW) and 1 MHz span. The signal-to-noise ratio (SNR) in the RF spectrum is higher than 70 dB, which indicates that the all-fiber laser system is in a very steady state, as shown in Fig. 9.

In conclusion, we demonstrate tunable femtosecond optical pulses from 1.6 to 2.32 μm based on SSFS in a silica-based highly nonlinear fiber with an all-fiber Er-doped laser system. The generated optical pulses can be used for Tm-doped fiber amplifier seeding to replace mode-locked Tm-doped fiber laser oscillators, usually more difficult to realize because of the relatively high anomalous dispersion of silica fibers in this wavelength range. In conjunction with the two stages of single-clad Tm-doped fiber amplifier without an external pulse compressor, we obtain a femtosecond optical pulse at 1.93 μm with a 32.9 MHz repetition frequency and 360 mW of output power correspond- ding to 105 kW peak power, providing an all-fiber laser system with a compact and versatile structure. Simultaneously, we believe that these tunable optical pulses may also be a good source of optically synchronized pump and seed pulses for amplifying systems based on Cr:ZnSe or Cr:ZnS.

## References

1. M. E. Fermann and I. Hartl, Nat. Photon. **7**, 868 (2013).
2. J. Nilsson and D. N. Payne, Science **332**, 921 (2011).
3. F. M. Mitschke and L. F. Mollenauer, Opt. Lett. **11**, 659 (1986).
4. J. H. Yuan, X. Z. Sang, C. X. Yu, X. W. Shen, K. R. Wang, B. B. Yan, Y. Han, G. Y. Zhou, and L. T. Hou, Chin. Phys. Lett. **29**, 104207 (2012).
5. R. Herda and O. G. Okhotnikov, in *Proceedings of Quantum Electronics and Laser Science Conference*, JWB39 (2005).
6. J. Walewski, M. Borden, and S. Sanders, Appl. Phys. B. **79**, 937 (2004).
7. N. Nishizawa and T. Goto, IEEE J. Sel. Top. Quantum Electron. **7**, 518 (2001).
8. D. Deng, T. Cheng, X. Xue, T. H. Tong, T. Suzuki, and Y. Ohishi, Proc. SPIE **9359**, 935903 (2015).
9. J. Takayanagi, T. Sugiura, M. Yoshida, and N. Nishizawa, IEEE Photon. Technol. Lett. **18**, 2284 (2006).
10. M. Y. Koptev, E. A. Anashkina, A. V. Andrianov, S. V. Muravyev, and A. V. Kim, Opt. Lett. **39**, 2008 (2014).
11. B. Tan, Z. Li, Z. Wang, C. Ge, D. Jia, W. Ni, and S. Li, Chin. Opt. Lett. **2**, 604 (2004).
12. B. Yan, J. Yuan, X. Sang, K. Wang, and C. Yu, Chin. Opt. Lett. **14**, 050603 (2016).
13. A. Andrianov, E. Anashkina, S. Muravyev, and A. Kim, Opt. Lett. **35**, 3805 (2010).
14. K. Kieu, R. Jones, and N. Peyghambarian, Opt. Express **18**, 21350 (2010).
15. N. Coluccelli, M. Cassinerio, A. Gambetta, P. Laporta, and G. Galzerano, Opt. Lett. **39**, 1661 (2014).
16. N. Coluccelli, M. Cassinerio, P. Laporta, and G. Galzerano, Opt. Lett. **38**, 2757 (2013).
17. G. Imeshev and M. Fermann, Opt. Express **13**, 7424 (2005).
18. J. Walewski, M. Borden, and S. Sanders, Appl. Phys. B. **79**, 937 (2004).
19. B. Jiao, J. Tian, X. Zhang, Y. Song, and L. Wang, Chin. Opt. Lett. **11**, S21901 (2013).